Structure and Stability of Short β-Peptide Nanotubes: A Non-Natural Representative of Collagen?

András Czajlik,[†] Tamás Beke,[†] Andrea Bottoni,[‡] and András Perczel*[,†,§]

Protein Modelling Group, HAS-ELTE Institute of Chemistry, Eötvös Loránd University, Pázmány Péter sétány 1/A, H-1117 Budapest, Hungary, Dipartimento di Chimica 'G.Ciamician', Università di Bologna, Via Selmi 2, 40126 Bologna, Italy, and Laboratory of Structural Chemistry and Biology, Institute of Chemistry, Eötvös Loránd University, Pázmány Péter sétány 1/A, H-1117 Budapest, Hungary

Received: December 5, 2007; Revised Manuscript Received: March 18, 2008; In Final Form: March 26, 2008

Since secondary structure elements are known to play a key role in stabilizing the 3D-fold of proteins for the design of non-natural proteins composed of β-amino acid residues, the construction of suitable secondary structural elements is mandatory. Folding analogues of α-helices and β-strands of β-polypeptides were already described (*Chem. Biodiversity* 2004, *1*, 1111[1]). Here, we present several collagen-like folds composed exclusively of β-Ala(s). Unlike their natural counterpart, these tubular nanostructures can be composed of more than three polypeptide chains aligned parallel and/or antiparallel. By using ab initio and DFT calculations we have optimized a large number of versatile collagen-like antiparallel nanostructures. In these tubular systems, oligopeptide strands are interconnected by $i \rightarrow (i)$ type H-bonds, except for the "closing" set. This latter is called "the H-bond zipper" and is either $(i) \rightarrow i$, $(i + 1) \rightarrow i$, or $(i + 2) \rightarrow i$ type. Antiparallel, tubular foldamers composed of l number of strands, each of k number of β-amino acid residues (e.g., ap(β-T$^{l}_{i+l})_k$, ap(β-T$^{l}_{i+1})_k$, or ap(β-T$^{l}_{i+2})_k$), are unexpectedly stable supramolecular complexes. Independent of k and l, the local backbone fold of the amino acid residues is usually spiral, abbreviated as "S_P" or "S^*_P". Nevertheless, in contrast to parallel, in antiparallel nanotubes the backbone fold can occasionally twist out from S_P or S^*_P type into an alternative local structure. However, the more the local geometry of the strands resembles to S_P or S^*_P, the higher the stability is. Besides the backbone twisting, the overall stability is determined by the type and the geometrical properties of the constituent H-bonds. Interestingly, higher number of total H-bonds can provide a lower overall stability, when H-bond parameters are inferior. In general, the increase of both the number of strands and their length stabilize the supramolecular complex. Now that, for β-peptides, collagen-like overall folds with their stability were determined, their POG- or PPG-like sequence specificity has to be revealed.

Introduction

β-peptides appear to be promising candidates as drug molecules and peptidomimetics.[3–6] Due to their additional backbone methylene group, they are considerably more resistant to proteolytic enzymes[7–9] and provide a more diverse side-chain chemistry[10] than the "natural" α-peptides. A number of topological and stereochemical studies have revealed interesting features of β-peptides, among others their basic backbone structural properties. The secondary structure elements formed by β-peptides were also investigated. Both experimental[11–19] and computational[20,21] studies revealed that β-peptides can adopt several conformers that are similar to the folding units of α-helices and β-strands. The latter type of conformer is composed of the slightly spiral $S_{P/M}$ (or **U4**)-type conformational building unit,[2,22,23] where $\varphi \approx -70°$, $\mu \approx 170°$, and $\Psi \approx 180°$. Although such a local folding unit can form β-sheet-like structures,[12–16,19,24,25] elongated multiple-stranded β-pleated sheets are not found in β-peptides like in the case of α-peptides (e.g., in silk or β-barrel type structures). On the contrary, both three- and four-stranded parallel systems composed of β-peptides were found to prefer a tubular shape to a β-layer.[2] Except for collagen, the tubular shape of α-peptides is uncommon. In fact, tube like structures were only described as aggregates of cyclic oligopeptides[26–29] and that of β-barrel proteins.[30–33]

According to quantum chemical studies, while multiple-stranded sheets composed of α-amino acid residues are stable and have low-energy structures those of β-peptides "roll-up" spontenously.[2] Although, these nanotubes have some similarity to β-barrels, they are much slimmer; even two β-peptides can self-assemble by forming a tube. These tubular systems can be rather regarded as non-natural representatives of tropocollagen. Tropocollagen is composed of three polypeptide chains, which self-assemble as a triple helix[34] and form subsequently a collagen, an essential extracellular protein of human body.[35] The triple helix is built up of polyproline II (or PPII in short) local folding units[34–36] with $\varphi \approx -70°$ and $\Psi \approx +150°$. Such an elongated backbone fold shows similarity to those typical of β-pleated sheets, where $\varphi \approx -150°$ and $\Psi \approx +150°$.

In the characterization of multiple-stranded supramolecular assemblies of α- and β-peptides, the following features should be considered. (i) Even though both are tubular, as many as eight or even more strands are required to form a β-barrel[31] while only three is required to make up tropocollagen. (ii) In a strand of a β-sheet, the orientation of the amide linkage

[†] Protein Modelling Group, Eötvös Loránd University.
[‡] Università di Bologna.
[§] Laboratory of Structural Chemistry and Biology, Eötvös Loránd University.
* To whom correspondence may be addressed. E-mail: perczel@chem.elte.hu. Telephone: 36-1-209-0555, ext.1653. Fax: 36-1-3722-620.

10.1021/jp7114803 CCC: $40.75 © 2008 American Chemical Society
Published on Web 06/10/2008

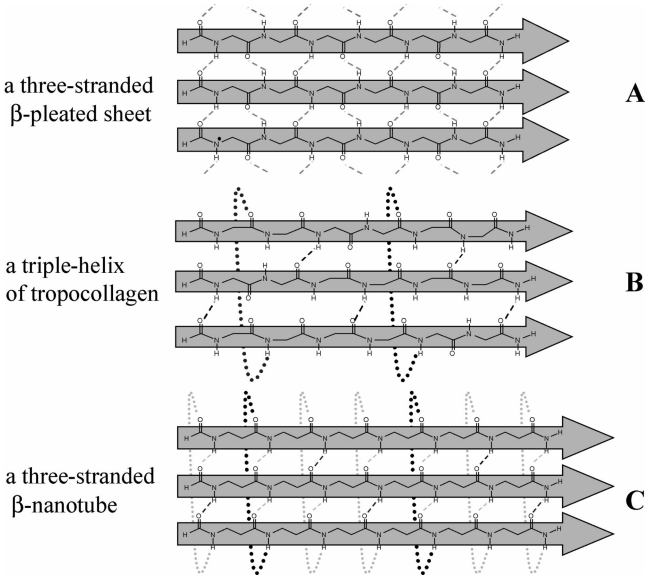

Figure 1. Schematic representation of a three-stranded β-pleated sheet (A), of a triple helix of tropocollagen (B), and of a three-stranded β-nanotube (C). The first two secondary structure elements are composed of α- while the third one of β-peptides, all aligned in parallel. Note that the H-bond pattern of tropocollagen (B) is tripled in a β-nanotube (C). (Hydrogen bonds are denoted with dashed line colored either by grey or by black.)

alternates monotonically (Figure 1A). In contrast, in a tropocollagen triple helix, the orientation of the amide groups involved in the interstrand H-bonds is uniform: a peptide strand only donates (N−H) hydrogen bond to the consecutive strand and only accepts (O═C) hydrogen bonds from the previous peptide strand (Figure 1B). Similarly, for parallel β-nanotubes the orientation of the amide groups in the hydrogen bonds is conserved (Figure 1C). (iii) In a parallel β-sheet, each peptide group is involved in two interstrand hydrogen bonds (Figure 1A). Only every third amide group is a hydrogen donor and another third is an acceptor in the H-bond network in tropocollagen (Figure 1B). The total number of hydrogen bonds strongly affects the stability, and thus a triple helix is expected to be less favored energetically over a β-sheet,[37] except for special primary sequences (e.g., POG, PPG). (iv) In a β-sheet, only the adjacent strands are connected by H-bonds (Figure 1A), while in a rolled-up nanotube, the "first" and the "last" strands are also linked (Figure 1B,C). Note that the H-bond pattern of tropocollagen (Figure 1B) is preserved and tripled in β-nanotubes (Figure 1C). Those H-bonds found in tropocollagen as well as β-nanotubes are denoted with black, and the additional H-bonds in β-tubular systems are shown with grey dashed lines in Figure 1.

Higher level ab initio and DFT calculations confirmed that the β-nanotube molecular assemblies are thermodynamically favored in vacuum.[2,38] The driving force of the tubular self-assembly could be on one hand the formation of optimum interchain H-bonds and on the other hand the adoption of locally optimum backbone structures. For β-peptides, three different types of superstructures were found, depending on the "tube-closing" hydrogen bond pattern (Figure 2). The intrinsic stability of these peptide nanotubes can be fine-tuned by using suitable side-chain arrangements resulting in polar-zippers, apolar-zippers, or amphipatic interactions. The analysis of the 3D-structure of parallel tubular systems has revealed that for four-stranded or larger nanotubes the inside diameter is large enough to incorporate guest molecules. Thus, these biocompatible peptide nanotubes could be rationally designed to fulfill different purposes such as novel biomaterials and selective drug protecting and drug delivering nanosystems.[28,29,39,40]

To achieve this goal, first, we need to understand the thermodynamic features of these tubular frameworks both for parallel, antiparallel, and mixed arrangements. The effect of side chains is ignored in this study, and thus all supramolecular scaffolds are composed of the simplest achiral β-amino acid residue, β-alanine.

Methods

Computational Details. All computations were carried out by using the Gaussian 03 software package.[40] Geometry optimizations were performed at the RHF/3−21G and B3LYP/6−31G(d) levels of theory for the $[CH_3-CO-(\beta\text{-Ala})_k-NHCH_3]_l$ model systems ($2 \le l \le 4$, $2 \le k \le 4$). To obtain the relative stability of nanotubes, the extended β-layers or β-sheets (β-E_l for short, with $2 \le l \le 4$) were optimized by using the following constraints: the first and the last nitrogen atoms of the first and last peptide strands are fixed to form a torsional angle equal to zero. To determine the energy associated with a nanotube formation from isolated single-stranded β-peptides, the most stable, zigzag type backbone-folds $(Z6_P)_4$ and $(Z6_P)_3$ of the parent β-peptide[2] (e.g., $-(\beta\text{-Ala})_4-$ and $-(\beta\text{-Ala})_3-$, respectively) were computed. Both the fully optimized nanotube and the reference structures were subjected to single point energy calculations carried out at the B3LYP/6−311++G(d,p)//B3LYP/631G(d) levels of theory (Table 1).

Nomenclature of the Nanotubes. A general short hand notation is introduced for nanotubes $[ap(\beta\text{-}T^l_i)_k$, $ap(\beta\text{-}T^l_{i+1})_k$, $ap(\beta\text{-}T^l_{i+2})_k]$ and the parental extended β-layers $[(\beta\text{-}E^l)_k]$, where "T" indicates tubular shape and "E" denotes extended-like β-sheet. To distinguish the parallel and the antiparallel nanotubes, the prefix "p" or "ap" is used. Superscript "l" stands for the total number of β-strands, while subscript "k" indicates the number of amino acid residues within a β-strand.

The subscript i, $i + 1$ or $i + 2$ characterizes the hydrogen bond pattern operative between the first and the last strands "closing" the nanotube, also called as the H-bond zipper (Figure 2). Subscript i is used when an H-bond is created between the ith amide group of the first and the ith amide group of the last strands. Similarly, abbreviation $i + 1$ or $i + 2$ is used when the ith amide group of the first peptide strand forms an H-bond with the $(i + 1)$th or the $(i + 2)$th amide group of the last strand, respectively. In all cases, we number the amide groups from one "end", namely, from the N-terminal of the first strand, independent of the orientation of the other strands (Figure 2). Thus, we can use the same type of H-bond nomenclature both for the antiparallel and the parallel nanotubes. Note that, according to the regular nomenclature, the type "i" H-bond is formed between the ith and $(i + 1)$th amino acid residues for a parallel, and ith and $(k - i)$th for an antiparallel arrangement.

Symbol (↑) and (↓) stands for the relative orientation of a strand. Thus, a fully parallel three-stranded system is denoted by ↑↑↑. For three-stranded antiparallel system $ap(\beta\text{-}T^3_{i+1})_k$ and $ap(\beta\text{-}T^3_{i+2})_k$, the subscript A, B, and C specifies the three different possibilities in relative orientations (Figure 3). Thus, A is of ↑↑↓-, B is of ↑↓↓-, and C is of ↑↓↑-type arrangement, where the closing set of hydrogen bonds appears between the first and the third strands (Figure 3).

Regardless of the side-chain composition, a β-peptide can adopt a maximum of 27 different local backbone folds, which were previously categorized as fully extended (a[a]a), elongated ($E_{M/P}$), spiral ($S_{M/P}$), zigzag ($ZX_{M/P}$), and helical ($HX_{M/P}$).[21] In

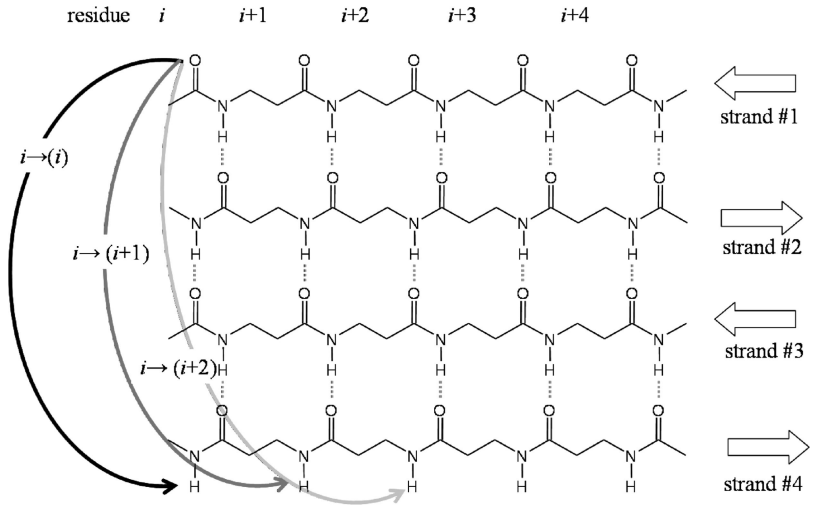

Figure 2. Type of H-bond zippers closing the nanotubes. Formation of the three different hydrogen bond patterns, $i \rightarrow (i)$, $i \rightarrow (i+1)$, or $i \rightarrow (i+2)$, between the first and the last strands of a four-stranded tubular structure resulting in ap(β-T^4_i)$_k$, ap(β-T$^4_{i+1}$)$_k$ and ap(β-T$^4_{i+2}$)$_k$ nanotubes. The H-bonds between the first and second, second and third, as well as between the third and fourth strands are denoted by dashed lines.

TABLE 1: Relative Stability, Dipole, and Hydrogen-Bond Parameters of the Four Amino Acid Long Antiparallel Nanotubes Computed at B3LYP/6-311++G(d,p)//B3LYP/6-31G(d) Level of Theory

type of nanostructure[a]	no. of interchain H-bonds[b]	d_{O-H}[c] (Å)	d_{N-O}[c] (Å)	α_{OHN} (deg)	dipole moment (D)	ΔE[d] (kcal mol^{-1})	ΔE[d]/tube closing H-bonds (kcal mol^{-1})	ΔE[e] (kcal mol^{-1})
3*(Z6$_p$)$_4$	12	-	-	-	-	-	-	**0.0**[h]
ap(β-E^3)$_4$	**0** + 10	**2.03**	**3.03**	**169.27**	**60.3**	**0.0**[f]	**0.0**	−0.4
[ap(β-T$^3_{i+1}$)$_4$]$_A$	**4** + 10	2.19	3.09	147.80	20.7	−6.5	−1.6	−6.9
[ap(β-T$^3_{i+2}$)$_4$]$_A$	**3** + 10	2.01	3.00	163.39	34.0	−17.4	−5.8	−17.8
[ap(β-T$^3_{i+1}$)$_4$]$_B$	**4** + 10	2.20	3.10	148.50	26.2	0.7	0.2	0.2
[ap(β-T$^3_{i+2}$)$_4$]$_B$	**3** + 10	2.01	2.98	159.67	32.4	−10.8	−3.6	−11.2
[ap(β-T$^3_{i+1}$)$_4$]$_C$	**4** + 10	2.13	3.05	150.16	28.4	−3.8	−1.0	−4.3
[ap(β-T$^3_{i+2}$)$_4$]$_C$	**3** + 10	2.02	3.01	162.30	37.3	−20.5	−6.8	−20.9
p(β-T$^3_{i+1}$)$_4$	**4** + 10	2.08[i]	2.99	149.79	21.7	−22.3	−5.6	−22.8
p(β-T$^3_{i+2}$)$_4$	**3** + 10	2.00	2.98	163.58	32.1	−31.8	−10.6	−32.3
4*(Z6$_p$)$_4$	16							**0.0**[i]
ap(β-E^4)$_4$	**0** + 15	**2.00**	**3.00**	**168.39**	**87.0**	**0.0**[g]	**0.0**	−19.3
ap(β-T^4_i)$_4$	**5** + 15	2.16	3.10	151.18	1.5	−18.6(−23.2)	−3.7	−37.9
ap(β-T$^4_{i+1}$)$_4$	**4** + 15	2.01	2.98	159.72	23.6	−30.1(−34.3)	−7.5	−49.4
ap(β-T$^4_{i+2}$)$_4$	**3** + 15	1.97	2.97	163.44	43.7	−26.8(−30.1)	−8.9	−46.1
p(β-T^4_i)$_4$	**5** + 15	2.05	2.98	150.73	2.2	−25.7	−5.1	−45.0
p(β-T$^4_{i+1}$)$_4$	**4** + 15	1.96	2.93	157.63	22.8	−41.8(−45.9)	−10.4	−61.1
p(β-T$^4_{i+2}$)$_4$	**3** + 15	1.95	2.95	166.63	36.3	−44.3(−47.5)	−14.8	−63.6

[a] For more on nomenclature, see Methods. [b] Total number of $i \rightarrow (i)$ type interchain hydrogen bonds between strands plus the number of hydrogen bonds closing the nanotubes in bold. [c] Average H···O and N(H)···O distances computed for the ensemble of interchain hydrogen bonds given in the second column. [d] Relative energies are compared with the extended-like β-sheet structures. Values in parenthesis are obtained at the X3LYP/6−311++G(d,p)//B3LYP/6−31G(d) level of theory. [e] Relative energies are computed with respect to (Z6$_p$)$_4$ and (Z6$_p$)$_3$, respectively. [f] E = −3714.682453 hartree. [g] E = −4952.939850 hartree. [h] E = −3714.681764 hartree. [i] E = −4952.909019 hartree. [j] For parallel nanotubes, the backbone and H-bond geometrical parameters as well as dipole moment values are taken from ref 2.

this notation subscript P stands for "plus" helicity and subscript M for "minus" helicity. In the case of the zigzag (Z) and helical (H) structures, intramolecular hydrogen bonds are present and X counts the number of atoms in one hydrogen bonded pseudo ring (e.g., *H*14). For the fully extended (a[a]a) conformation, the short hand notation "A" is introduced.

Although in some cases the dihedral angles of the residues considerable differ from each other, nevertheless, for the description of the backbone conformation of the strands, the average backbone fold (e.g., S$_P$) is used. This can be done since usually the same local fold, e.g., S$_P$, E, a[a]a)[21] is found throughout a strand, regardless of its length.

The inside diameters were determined by using the *i*th C$^\alpha$ atoms of the individual strands for the collagen-like and β-nanotubes. In the case of the three-stranded tubular systems, these atoms form a closely equilateral triangle, and based on this, a three-point circle can be drawn and its diameter used as diameters of tubes.

Results and Discussion

Precision and Accuracy. Our first goal was to determine the effect of the level of theory applied on structure and stability. Conformational data of the individual models obtained by geometry optimization at the RHF/3−21G and at the B3LYP/6−31G(d) levels of theory were compared. We found that the backbone dihedral angles of the nanotubes are similar at both levels of theory (Tables 2 and S1, S2, and S3 of Supporting Information). In the case of the four-stranded model systems the difference between the corresponding φ, μ, Ψ, and ω values (Figure 4) is less than 10° with the single exception of ap(β-T$^4_{i+2}$)$_3$ (Table S3). For three-stranded tubular systems, most of the dihedral angles do not vary as a function of the level of

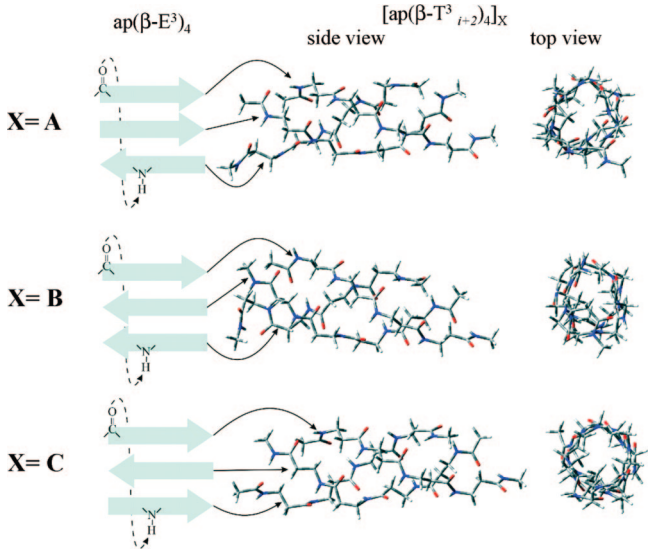

Figure 3. Schematic backbone arrangement of the extended reference structure, ap(β-E^3)$_4$ by arrows, and the "rolled up" 3D conformer of the three-stranded tubular system (wireframe): side and top views. A total of three different types of three-stranded superstructures were obtained, **A** = [ap(β-T$^3_{i\,+\,2}$)$_3$]$_A$, **B** = [ap(β-T$^3_{\,i\,+\,2}$)$_3$]$_B$, and **C** = [ap(β-T$^3_{\,i\,+\,2}$)$_3$]$_C$, where the "closing" $i \rightarrow i + 2$ H-bond zipper occurs between the first and the third strands.

theory applied, nevertheless, some of them differ from each other by some 20° or 30°. For example, for ap[(β-T$^3_{\,i\,+\,2}$)$_3$]$_A$, the average φ value of the second strand is −140° at the RHF/3−21G and −178° at the B3LYP/6−31G(d) level of theory. Even though an RHF optimization on a small split-valence basis set usually provides acceptable structural properties for models composed of as many as 92 heavy atoms, the geometrical properties calculated at B3LYP/6−31G(d) level of theory are used throughout this paper.

The second question to be addressed was to find the adequate measure of relative stability. It was shown earlier[42] that for noncovalently attached peptide dimers stability values expressed in ΔE and ΔG correlate significantly ($R^2 > 0.9$) at the B3LYP/6−311++G(d,p) level of theory. In addition, we have found for β-peptides adopting S$_{P/M}$ local folds that ΔH dominates the ΔG term.[22] Thus, the more "economic" stability measure, ΔE, can be used for ranking nanotube stabilities at an acceptable level of accuracy.

Third, the magnitude of basis set superposition error, BSSE, at the B3LYP/6−311++G(d,p) level of theory was found for parallel β-peptides to be in the range of chemical accuracy (∼1.0 kcal mol^{-1}).[2] Thus, no explicit BSSE calculations were carried out for these β-nanotubes.

Structural Diversity of the Antiparallel Nanotubes and of the Parent β-Sheets. Similarly, as found for parallel systems,[2] the three- and four-stranded antiparallel β-layers can only be obtained when planarity conserving constraint(s) are used during structure optimization (see Methods). By interacting with each other, the individual β-strands form a large variety of tubular nanosystems (Figures 2, 3, and 5). Note that when odd number of β-strands are involved in a tube, due to their "rolled-up" nature, even in an "antiparallel" nanotube, two out of the three strands must be parallel with respect to each other, called as "mixed" alignment or packing mode. As a consequence of it, ↑↑↓-type (A), ↑↓↓-type (B), and ↑↓↑-type (C) structures can be distinguished (Figure 3). In contrast to this, in four-stranded tubular structures, the alignment of the strands can be purely antiparallel (Figures 2 and 5).

Typically, the interchain connecting hydrogen bonds are of $i \rightarrow (i)$ type. However, the "tube closing" H-bond pattern, also called as the "H-bond zipper", could be of $i \rightarrow (i)$, $i \rightarrow (i + 1)$, and $i \rightarrow (i + 2)$ type. Note that in the antiparallel structures the hydrogen bonds could be hardly defined by the regular notation, i.e., when i, $i + 1$, $i + 2$, etc., refer to the amino acid residues, and thus in this study, these symbols refer to the amide groups counted from one direction (N-terminal of the first strand), irrespective of the orientations of the peptide chains (Figures 2 and 5). This way the topology of the H-bond zippers are similar both in parallel and antiparallel tubes. The different H-bond zippers result in the ap(β-T^l_i)$_k$, ap(β-T$^l_{i+1}$)$_k$, and the ap(β-T$^l_{i+2}$)$_k$ type tubular nanosystems ($2 \le l \le 4$ and $2 \le k \le 4$). For four-stranded antiparallel systems, all three types of H-bond zippers, ap(β-T^4_i)$_k$, ap(β-T$^4_{i+1}$)$_k$, and the ap(β-T$^4_{i+2}$)$_k$ were optimized (Table 1). For three-stranded nanotubes, the A, B, and C variants with the three different type of H-bond zippers can result in a total of nine different type of nanotubes, ap(β-T$^3_{i+j}$)$_k$, where j = 0, 1 and 2. By structure optimization, six out of the nine were found, ap(β-T$^3_{i+1}$)$_k$ and ap(β-T$^3_{i+2}$)$_k$, since no ap(β-T^3_i)$_k$ type was obtained. For the two-stranded nanotubes, a total of three antiparallel systems were expected, ap(β-T^2_i)$_k$, ap(β-T$^2_{i+1}$)$_k$, and ap(β-T$^2_{i+2}$)$_k$, but none could be optimized. All this signals that besides the preferable local backbone fold (*e.g.* S$_P$ or S*$_P$) the number of the strands also determines the overall stability of these nanotubes.

Structure and Stability of the Antiparallel and Parallel Four-Stranded Nanotubes. As expected, all four-stranded nanotubes have a greater stability than the "flattened" ap(β-E^4)$_k$ type superstructures. The surplus stability of the tubes is derived from the roll-up, when "extra" hydrogen bonds form. For example, with respect to the "flat" ap(β-E^4)$_4$ structure, which consists of a total of 15 H-bonds, the ap(β-T^4_i)$_4$ nanotube forms 5 additional H-bonds, resulting in a total of 20. Thus, the obtained energy difference, ΔE= −18.6 kcal mol^{-1}, between the above two supramolecular complex at B3LYP/6−311++G(d,p) level of theory seems to be reasonable, reflecting to an average stability of ∼3.7 kcal mol^{-1}per H-bond.

As mentioned above, a β-peptide can form a maximum of 27 different local backbone folds, categorized as fully extended (A), elongated (E$_{M/P}$), spiral (S$_{M/P}$), zigzag (ZX$_{M/P}$), and helical (HX$_{M/P}$).[21] In parallel tubular systems, the central type of conformational element is the spiral backbone fold, S$_P$, where subscript P stands for its "plus" helicity. All four chains of a four-stranded parallel nanotube, regardless of the length of the component, polypeptides adopt exclusively S$_P$ local backbone structure (ref 2 and Table 2). Its appropriate φ, μ, and Ψ values (Figure 4) are in the vicinity of g-[a]a with $\varphi \approx -90°$, $\mu \approx 180°$, and $\Psi \approx 180°$.[22] In the case of the most stable four-stranded antiparallel nanotubes, ap(β-T$^4_{i+2}$)$_k$ and ap(β-T$^4_{i+1}$)$_k$, all amino acid residues in the (↑) strands adopt an S_P while those in the (↓) strands (see Methods) have an S*$_P$ backbone fold (Figure 5 and Table 2). Note that while an S$_P$ conformer has dihedral angles φ[μ]Ψ = g-[a]a an S^*_Pfold is composed of φ[μ]Ψ = a[a]$g-$, signaling their complementing or mirror image nature. Therefore, when reading out the conformation of the (↓) strands not from the conventional N- to C-terminal but from the unusual C- to N-terminal direction, the conformation code of all four β-strands become S$_P$S$_P$S$_P$S$_P$. Thus, even though two strands are reversed in an antiparallel nanotube with respect to the "all-parallel" system, both the overall fold and the relative packing of the strands are similar. In contrast to ap(β-T$^4_{i+2}$)$_k$ and ap(β-T$^4_{i+1}$)$_k$, the ap(β-T^4_i)$_k$ type nanosystem is composed of S$_P$ (↑) and A (↓) local backbone structures. Such

TABLE 2: Type of β-Ala Backbone Conformers in Four Amino Acid Long Antiparallel and Parallel Nanostructures with the Relative Stability of the Supramolecular Complexes as Computed at B3LYP/6-31G(d) Level of Theory[a]

type of nanostructures[a]	typical conf. code[a] of strand #1	typical conform. code[a] of strand #2	typical conform. code[a] of strand #3	typical conform. code[a] of strand #4	ΔE^b (kcal mol^{-1})
ap(β-E^3)$_4$	A (↑)	S_M (↓)	A (↑)		0.0
[ap(β-T$^3_{i+1}$)$_4$]$_A$	S_P (↑)	S_P (↑)	S^*_P (↓)		−6.5
[ap(β-T$^3_{i+2}$)$_4$]$_A$	S_P (↑)	S^*_P (↑)	E_P (↓)		−17.4
ap(β-T$^3_{i+1}$)$_4$]$_B$	S_P (↓)	S^*_P(↑)	A (↑)		0.7
ap(β-T$^3_{i+2}$)$_4$]$_B$	S_P (↓)	$Z6^*_p$ (↑)	A (↑)		−10.8
[ap(β-T$^3_{i+1}$)$_4$]$_C$	S_P (↑)	S^*_P (↑)	A (↓)		−3.8
[ap(β-T$^3_{i+2}$)$_4$]$_C$	S_P (↑)	S_P (↑)	A (↓)		−20.5
p(β-T$^3_{i+1}$)$_4$	S_P (↑)[c]	S_P (↑)	S_P (↑)		−22.3
p(β-T$^3_{i+2}$)$_4$	S_P (↑)	S_P (↑)	S_P (↑)		−31.8
ap(β-E^4)$_4$	E_M (↓)	A (↑)	S_M (↓)	A (↑)	0.0
ap(β-T^4 $_i$)$_4$	A (↑)	S_P (↓)	A (↑)	S_P (↓)	−18.6
ap(β-T^4 $_{i+1}$)$_4$	S_P (↑)	S^*_P (↓)	S_P (↑)	S^*_P (↓)	−30.1
ap(β-T^4 $_{i+2}$)$_4$	S^*_P (↑)	S_P (↓)	S^*_P (↑)	S_P (↓)	−26.8
p(β-T^4 $_i$)$_4$	S_P (↑)	S_P (↑)	S_P (↑)	S_P (↑)	−25.7
p(β-T^4 $_{i+1}$)$_4$	S_P (↑)	S_P (↑)	S_P (↑)	S_P (↑)	−41.8
p(β-T^4 $_{i+2}$)$_4$	S_P (↑)	S_P (↑)	S_P (↑)	S_P (↑)	−44.3

[a] Local backbone conformational codes (e.g., S_P, a[a]a, E_M)[33] of the constituent amino acid residues are always the same along a strand. For example, for the tetrapeptide Ac−(β-Ala)$_4$−NHCH$_3$, the homoconformer S_P stands for the repeat of four consecutive S_P local folds or $(S_P)_4$ for short. Fully extended (a[a]a) conformation is labeled here as "A". Symbol (↑) and/or (↓) indicates the relative orientation of the strands, and thus for a four-stranded parallel nanotube, all strands are oriented uniformly (e.g., (↑), (↑), (↑), (↑)), while for an antiparallel arrangement, the (↑), (↓), (↑), (↓) symbol is used. [b] Relative energies are compared to the antiparallel extended-like β-sheet structures [ap(β-E^i)$_j$]. [c] For parallel nanotubes the local backbone folds are determined in ref 2.

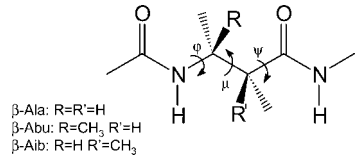

Figure 4. A typical backbone subunit of a β-peptide, where local conformation is determined by the φ, μ, and Ψ dihedral angles.

a conformational change seems to be required for the formation of H-bonds (details see later). As the consequence of this local distortion, the stability of the ap(β-T^4_i)$_k$ type nanotubes has decreased: ΔE(ap(β-T^4_i)$_4$ = −18.6 kcal mol^{-1} ≫ ΔE(ap(β-T$^4_{i+2}$)$_4$ = −26.8 kcal mol^{-1} > ΔE(ap(β-T$^4_{i+1}$)$_4$ = −30.1 kcal mol^{-1}.

The stability of a tubular system is also influenced by its closing H-bond pattern. Although the ap(β-T$^4_{i+2}$)$_4$ and ap(β-T$^4_{i+1}$)$_4$ superstructures have less H-bonds (19 and 18, respectively) than that of ap(β-T^4_i)$_4$, they have a considerably lower energy. This can partly be explained by the differences of their local backbone fold. Higher stability can also be gained even for a system equipped with fewer H-bonds, if the conformational properties of the H-bonds have improved. In ap(β-T^4_i)$_4$, the length of O···H distances are longer by ∼0.15 Å than they are in the ap(β-T$^4_{i+1}$)$_4$ superstructure, where d_{O-H} is 2.01 Å. Furthermore, the H-bond angles, α_{O-H-N}, have also more favorable values ($\Delta\alpha \approx 8°$) in the latter type of nanotube (Table 1). Nanotube ap(β-T$^4_{i+2}$)$_4$, which has only 18 hydrogen bonds, also shows considerably more favorable H-bond parameters (shorter d(s), $\Delta d \sim 0.18$ Å, and better H-bond angles, $\Delta\alpha \approx 11.5°$) than that of ap($\beta$-T$^4_i$)$_4$. It means that the ap($\beta$-T$^4_{i+1}$)$_4$ and ap(β-T$^4_{i+2}$)$_4$ tubular systems not only adopt the preferred $S_PS^*_PS_PS^*_P$ local backbone fold but also their H-bonds have an almost ideal geometrical properties. A very similar result is obtained when comparing the H-bond parameters of the shorter ap(β-T^4_i)$_3$, ap(β-T$^4_{i+1}$)$_3$ and ap(β-T$^4_{i+2}$)$_3$ type nanotubes (Table S4 of Supporting Information). Thus, ap(β-T^l_i)$_k$ tubular systems are sterically less favored, having significantly weaker H-bonds compared to the other type of nanotubes.

The ap(β-T$^4_{i+1}$)$_4$ has the lowest relative energy among all type of antiparallel superstructures. It shows rather similar structural and H-bond properties as ap(β-T$^4_{i+2}$)$_4$, but this nanotube forms 19 hydrogen bonds instead of 18. Thus, we concluded that, similar to the parallel nanotubes, the stability of the antiparallel superstructures strongly depend both on the local backbone fold of the component β-amino acid residues and on the geometrical properties of the contributing H-bonds.

The previously characterized parallel systems[2] formed of "all S_P" backbone conformational units proved to be the most stable supramolecular complexes. Their overall stability is fine-tuned by the H-bond zipper of type $i \rightarrow (i)$, $i \rightarrow (i+1)$ or $i \rightarrow (i+2)$, resulting in the following order of stability: ΔE(p(β-T^4_i)$_4$ < ΔE(p(β-T$^4_{i+1}$)$_4$ < ΔE(p(β-T$^4_{i+2}$)$_4$. None of the antiparallel nanotubes are as stable as the analogous parallel system: e.g., ΔE(p(β-T$^4_{i+1}$)$_4$ = −41.8 kcal mol^{-1} < ΔE(apβ-T$^4_{i+1}$)$_4$ = −30.1 kcal mol^{-1}. Seemingly, the conformational differences, $S_PS_PS_PS_P$ and $S_PS^*_PS_PS^*_P$ (or S_PAS_PA), are the reason of the above described stability difference. Furthermore, the dissimilar orientation of their amide bonds results in interchain H-bonds of different strengths. Finally, in the parallel nanotubes, the length of O···H distances are significantly shorter ($\Delta d \sim 0.09$ Å) than they are in the antiparallel tubular systems, especially for (β-T^4_i)$_k$. These differences altogether are made responsible for the lower stability of the antiparallel systems, $\Delta\Delta E$ = −11.7 kcal mol^{-1}, spelled out above.

Structural and Energetic Properties of the Antiparallel Three-Stranded Nanotubes. As found for the four-stranded, the parallelly aligned systems are the most stable also for the three-stranded nanotubes (e.g., ΔE(p(β-T$^3_{i+2}$)$_4$= −32.3 kcal mol^{-1} < ΔE[ap(β-T$^3_{i+2}$)$_4$]$_C$ = −20.5 kcal mol^{-1}), resulting in the "all S_P" overall fold (Tables 1, 2, and S1 of Supporting Information). This underlines that the S_P local conformation is the ideal fold for parallel β-nanotubes. As mentioned above, for the three-stranded antiparallel nanotubes beside the A, B, and C variants (see above), two types of H-bond zippers, ap(β-T$^3_{i+1}$)$_k$ and ap(β-T$^3_{i+2}$)$_k$, were found (Methods and Figure 3). Their structural and energetic properties are predominantly influenced by their "mixed" (i.e., antiparallel−parallel) nature. In the case of three-stranded nanotubes, the local conformation should be S_P for the two (↑) and S^*_P for the third (↓) strand.

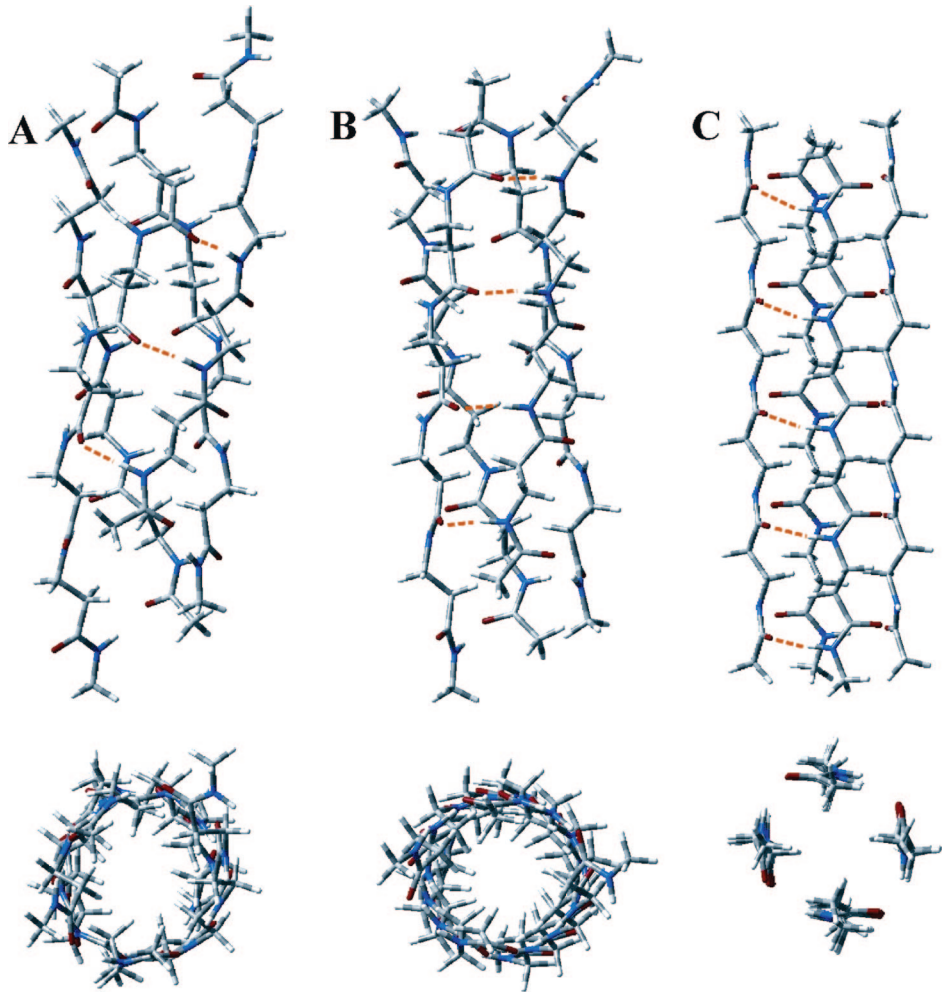

Figure 5. Four-stranded nanotubes, **A** = ap(β-T$^4_{i+2}$)$_4$, **B** = ap(β-T$^4_{i+1}$)$_4$, and **C** = ap(β-T^4_i)$_4$, with the three different H-bond zipper types, $i \rightarrow (i + 2)$, $i \rightarrow (i + 1)$, and $i \rightarrow (i)$ (labelled with orange dashed lines).

Such a nanotube composed of only these locally "ideal" building units is analogous to that of the "all S_P" described for fully parallel tubular systems. Due to formation of non-ideal H-bonds, some local backbone structural distortion(s) can occur. In such cases, the conformation of some building units shifts from the ideal S^*_P or S_P to A or E_P etc., (Table 2). Unlike for four-stranded antiparallel systems, where locally "ideal" conformers are present (e.g., ap(β-T$^4_{i+1}$)$_4$), for three-stranded tubes, only [ap(β-T$^3_{i+1}$)$_4$]$_A$ showed such perfect parameters. Except from the latter nanotube, where S_P for (↑) and S^*_P for (↓) is found, the three-stranded tubes contain some more or less locally distorted backbone units. This holds for systems composed of tri- as well as tetrapeptides (Tables 1, 2, and S4 and S5 of Supporting Information). Therefore, only the longer tubular systems are discussed in details.

In the case of ap(β-T$^3_{i+2}$)$_4$, the geometrical properties of the H-bond do not differ significantly in any of its subtypes: [ap(β-T$^3_{i+2}$)$_4$]$_A$, [ap(β-T$^3_{i+2}$)$_4$]$_B$, and [ap(β-T$^3_{i+2}$)$_4$]$_C$. In fact, variation of the H-bond parameters is marginal: $\Delta d < 0.02$ Å and $\Delta\alpha < 3°$. If so, then the backbone geometrical properties of the nanotubes must be responsible for their dissimilar stability. The most stable system [ap(β-T$^3_{i+2}$)$_4$]$_C$ ($\Delta E = -20.5$ kcal mol^{-1}) has the least distorted S_PS_PA local structure, where only the (↓) strand has a "non-ideal" local fold. Note that the backbone fold in subtypes A and B of ap(β-T$^3_{i+2}$)$_4$ are considerably different of the ideal $S_PS_PS^*_P$ structure: S_PZ6_PA for [ap(β-T$^3_{i+2}$)$_4$]$_B$ and $S_PS^*_PE_P$ for [ap(β-T$^3_{i+2}$)$_4$]$_A$. This makes their overall stability lower {ΔE[(ap(β-T$^3_{i+2}$)$_4$]$_B$) = −10.8 kcal mol^{-1} and ΔE([ap(β-T$^3_{i+2}$)$_4$]$_A$) = −17.4 kcal mol^{-1}} than that of [ap(β-T$^3_{i+2}$)$_4$]$_C$ ($\Delta E = -20.5$ kcal mol^{-1}) (Tables 1 and 2). Clearly, the local distortion of the constituent strands has a "price" to pay in terms of energy.

The stability of ap(β-T$^3_{i+1}$)$_k$ (i.e., [ap(β-T$^3_{i+1}$)$_4$]$_A$, [ap(β-T$^3_{i+1}$)$_4$]$_B$, and [ap(β-T$^3_{i+1}$)$_4$]$_C$) equipped with an $i \rightarrow (i + 1)$ type H-bond zipper is also determined by its local backbone fold. As in [ap(β-T$^3_{i+1}$)$_4$]$_A$, the backbone fold is close to ideal, S_P for (↑) and S^*_P for (↓), and this nanotube has the lowest relative energy among all $(i + 1)$ type three-stranded systems composed of tetrapeptides ($\Delta E = -6.5$ kcal mol^{-1}). In contrast to this, ap(β-T$^3_{i+1}$)$_4$]$_B$ adopts S^*_P and "A" for the two (↑) and S_P conformation for the third (↓) strand. As all three polypeptide chains are strongly affected, the overall electronic energy increases ($\Delta E = +0.7$ kcal mol^{-1}) (Table 2).

Comparison of the total number of H-bonds with the relative stability of the three-stranded nanotubes, ap(β-T$^3_{i+1}$)$_k$ and ap(β-T$^3_{i+2}$)$_k$, makes it clear again that a higher number of H-bonds does not necessary imply a lower relative energy. The ap(β-T$^3_{i+2}$)$_4$ tubular systems contain less H-bonds, a total of 13, than ap(β-T$^3_{i+1}$)$_4$ superstructures do (Table 1), however, the former type of nanotubes have a considerably higher stability ($\Delta\Delta E >$ 10 kcal/mol). For example, the relative stability of [ap(β-T$^3_{i+2}$)$_4$]$_A$ ($\Delta E = -17.4$ kcal mol^{-1}) is significantly higher than that of [ap(β-T$^3_{i+1}$)$_4$]$_A$ ($\Delta E = -6.5$ kcal mol^{-1}) (Table 1). A system containing a lower number of total H-bonds can only

be more stable if its structural parameters (e.g., those of the hydrogen bonds) are superior. In fact, the O···H distances are longer ($\Delta d = 0.15 \pm 0.03$ Å) and the H-bond angles are more tilted ($\Delta\alpha = 13 \pm 1.6°$) in those structures that otherwise have a higher number of closing H-bonds (Table 1). Decreasing the length of the component polypeptide chains makes no difference. This explains why only the ap(β-T$^3_{i+2}$)$_k$ type nanotubes, having less number but more optimal H-bonds, show a considerable higher stability with respect to that of the extended-like β-layer (β-E^3)$_k$. In fact, the H-bond geometrical properties of ap(β-T$^3_{i+1}$)$_k$ is unfavorable, and consequently both [ap(β-T$^3_{i+1}$)$_k$]$_A$ and [ap[(β-T$^3_{i+1}$)$_k$]$_C$ have just slightly greater stability than that of (β-E^3)$_k$ (Table 1). Moreover, [*ap*(β-T$^3_{i+1}$)$_4$]$_B$ has so poor H-bond parameters (longer O···H distances, $\Delta d =$ 0.17 Å, and worse H-bond angles, $\Delta\alpha = 20.7°$) that its relative energy is even higher (+0.7 kcal mol^{-1}) than that of (β-E^3)$_4$.

Stability of the Antiparallel and Parallel β-Nanotubes as a Function of the Environment, Chirality, Number of H-Bonds, and Peptide Strands. Stability analysis of the antiparallel nanotubes as function of the number of "closing" H-bonds was also performed. As expected, increase of the length of the polypeptide chains in nanotubes results in more stable superstructures. Furthermore, in the case of four-stranded tubular structures, the energy values perfectly correlate with the number of H-bonds present in the H-bond zipper (Table 1). For example, the energy gain is 22.3 kcal mol^{-1} for the ap(β-T$^4_{i+1}$)$_3$ and 30.1 kcal mol^{-1} for ap(β-T$^4_{i+1}$)$_4$. By calculating the relative stability per "closing" H-bond, we got 7.4 kcal mol^{-1} for the shorter and 7.5 kcal mol^{-1} for the longer nanotube. The same similarity holds for ap(β-T^4_i)$_k$ and ap(β-T$^4_{i+2}$)$_k$ as well as for most three-stranded tubular systems (Tables 1 and S4 of Supporting Information). This observation seems general except that of the C-type three-stranded tubes. Here, both the geometrical and H-bond properties of the four- and of the three-amino acid long systems are considerably different, making the comparison unrealistic. This stability match indicates that the increasing stability of a longer nanotube is coming from the increasing number of "closing" H-bonds.

As mentioned earlier, the type of "closing" H-bond and the ideality of the local backbone fold make a difference between the stability of tubular systems. Therefore, ap(β-T$^4_{i+2}$)$_k$, which has geometrical parameters the closest to the ideal values, show the highest energy gain per H-bond: $\sim 8.8 \pm 0.1$ kcal mol^{-1}. In contrast to this, the stabilization gained per "closing" H-bonds for ap(β-T^4_i)$_4$ system, which possesses sterically less favored H-bonds, are just about 3.7 kcal mol^{-1}. Thus, the stabilization energy gained per H-bond could be doubled if structural parameters had improved (Table 1).

In general, increasing the number of the strands of the nanotube makes the nanostructure more stable. For example, while the relative energy of ap(β-T$^3_{i+1}$)$_4$ types tubular systems varies between +1 and −7 kcal mol^{-1}, that of ap(β-T$^4_{i+1}$)$_4$ is −30.1 kcal mol^{-1}. Such a huge difference between the stability of the three- and four-stranded nanotubes can not be explained by the increased number of H-bonds. In fact, there are two additional factors to be considered. (i) The local fold in ap(β-T$^4_{i+1}$)$_4$ is very favorable, $S_PS^*_PS_PS^*_P$. (ii) The widening of the tubular system improves the geometrical parameters of the H-bonds. Even for the most stable [ap((β-T$^3_{i+1}$)$_4$]$_A$, the O···H distances are 2.19 Å and the α_{O-H-N} angles are 147.8°. In the corresponding four-stranded tubular system, ap(β-T$^4_{i+1}$)$_4$, the O···H distances are shorter (2.01 Å) and its H-bond angles are better (159.7°). In conclusion, increasing the number of the strands in a nanotube introduces a considerable amount of stability as long as the structural parameters improve.

To test the effect of environment on the affinity of tube formation, selected systems were subjected to preliminary calculations using a continuum solvent model.[43] Several calculations were accomplished for both parallel and antiparallel four-stranded β-nanotubes using the integral equation formalism polarizable continuum model (IEFPCM))[42,43] with implicit solvent−water, acetonitrile, and heptane at the B3LYP/6−311++G(d,p)//B3LYP/6−31G(d)) level of theory. First, as expected, the parallel systems are always significantly more stable than the antiparallel tubular structures. Second, we found that the higher stability of the nanotubes compared to the extended-like β-layer is preserved only in environment of low dielectric constant, i.e, using implicit heptane ΔE(ap(β-T$^4_{i+1}$)$_4$ = −7.6 kcal mol^{-1} and ΔE(p(β-T$^4_{i+2}$)$_4$ = −23.7 kcal mol^{-1}. In contrast, in polar solvent system (water), the tubular structures are less favored (Table S6 of Supporting Information). Even the relative energy of the most stable parallel nanotube [(p(β-T$^4_{i+2}$)$_4$] is considerably higher (+8.5 kcal mol^{-1}) than that of its extended-like β-layer counterpart [(β-E^4)$_4$]. Moreover, in the case of antiparallel nanotubes the energy difference between the tubular and the flattened systems is very high: ΔE(ap(β-T^4_i)$_4$ = +44.8 kcal mol^{-1} ≫ ΔE(ap(β-T$^4_{i+1}$)$_4$ = +28.9 kcal mol^{-1} > ΔE(p(β-T$^4_{i+2}$)$_4$ = +22.5 kcal mol^{-1}. When using semipolar implicit solvent (acetonitrile), the relative energy distribution is similar to the case of water (Table S6 of Supporting Information). These results are in line with the expectations, because in nanotubes, the most polar amide groups participate in the interchain H-bonds and thus these molecules could keep their hydrogen bonding pattern much easier in an apolar external matrix. Thus, it is proposed that such peptide nanotubes form only in apolar (e.g., membrane) environment. Interestingly enough, although the extended-like β-layers have less free amide groups than the one-stranded zigzag type structures, they are significantly more stable in water ($\Delta\Delta E \sim 20$ kcal mol^{-1}). Note, however, that this phenomenon could be derived from various reasons including the inadequacy of the applied implicit solvent model. Thus, further extensive investigations are needed using solvent models to determine the stability properties of these structures, which is beyond the scope of this study.

Recently it is proposed that current density functional theory methods using gradient corrected functionals are inadequate to describe van der Waals interactions.[44−46] Because van der Waals contribution could significantly shift the relative stability distribution even in the achiral models used in this study, test calculations were performed using the X3LYP functional, which was developed recently to improve description of van der Waals (vdW) interactions and hydrogen bonds in biomolecules.[47] Thus, single point energy calculations were performed on six structures: ap(β-E^4)$_4$, ap(β-T^4_i)$_4$, ap(β-T$^4_{i+1}$)$_4$, ap(β-T$^4_{i+2}$)$_4$, p(β-T$^4_{i+1}$)$_4$, and p(β-T$^4_{i+2}$)$_4$ at the X3LYP/6−311++G(d,p)//B3LYP/6−31G(d) level of theory. Results show a ∼3−4 kcal/mol^{-1} additional stabilization for each of the five tubular systems (Table 1). These preliminary calculations propose that vdW interaction has a slight stabilizing effect on such tubular frameworks. Note that larger side chains would definitely have a larger vdW contribution to the relative energy of the various structures.

Finally, our preliminary studies show, that the nanotubes composed of two chiral β-peptides, namely, β-Abu and β-Aib, respectively, also prefer the β-nanotube molecular assemblies in vacuum. Examining the geometry of these chiral molecules,

we found that their backbone fold depend on position of the methyl side-chain. Those parallel nanotubes which contain β-Abu residues, adopt exclusively S_P local backbone structure. Their average backbone dihedral angles ($\langle\varphi\rangle = 84.7$, $\langle\mu\rangle = 173.9$, $\langle\Psi\rangle = 151.8$, and $\langle\omega\rangle = 172.9$) are very similar to those found in achiral β-nanotubes (Table S1 of Supporting Information). In contrast, although superstructures composed of β-Aib residues also formed tubular systems, due to the unfavorable orientation of the methyl groups, they have locally distorted backbone units. Only two of the three peptide chain can be characterized as the same local fold (S^*_P and A, respectively) for all amino acid residues (Table S1 of Supporting Information). In contrast, the residues of the third strand adopt three totally different S_P-, S_M-, and A-type backbone conformations. It means that these nanotubes have a "non-ideal" backbone structure. In consequence, β-Aib residues form considerably less stable tubular systems (for p(β-T^3_{i+2})$_3$models $\Delta\Delta E \sim 20$ kcal mol^{-1}) than the tubes composed of β-Abu amino acids.

Incorporation of Small Molecules into Nanotubes. The ability of binding guest molecules was computationally tested. Three- and four-stranded nanotubes were optimized at the RHF/3−21G level of theory with water and acetonitrile molecules inside. Results indicate that only larger nanotubes (e.g., ap(β-T^4_{i+1})$_4$ and ap(β-T^4_{i+2})$_4$) can host water and acetonitrile. Tubular systems composed of three peptide chains are too tight and even small molecules disintegrate the characteristic H-bond network of the nanosystem. As an example of longer and apolar guest, an unbranched C20 alkane (i.e., icosane) was pulled inside the four-stranded p(β-T^4_{i+1})$_3$ and p(β-T^4_{i+2})$_3$ type nanotubes. Even though the fully optimized host−guest complex can be obtained, its stability is expected to be low. At B3LYP/6−31+G(d,p) level of theory, the interaction-energy ($\Delta E_{int} = \Delta E_{complex} - [\Delta E_{host} + \Delta E_{guest}]$) of all the three guest molecules is positive. For the acetonitrile placed in ap(β-T^4_{i+1})$_4$ and ap(β-T^4_{i+2})$_4$ nanotubes, the destabilization energy is as large as +17.8 and +11.3 kcal mol^{-1}, respectively. The situation improves with the more polar water molecule placed in the ap(β-T^4_i)$_4$, ap(β-T^4_{i+1})$_4$, and ap(β-T^4_{i+2})$_4$ nanotubes: $\Delta E_{int} = +1.0$, +1.7, and 6.7 kcal mol^{-1}, respectively. For icosane, destabilization seems to be again large enough: +22.6 and +35.5 kcal mol^{-1} for the p(β-T^4_{i+1})$_3$ and p(β-T^4_{i+2})$_3$ nanotubes, respectively. We found that due to icosane binding the conformation of all strands shifts from the ideal S_P to A in the p(β-T^4_{i+2})$_3$ tubular system. Since the stability of this host−guest complex is very low (+35.5 kcal mol^{-1}), it shows again that the energy of the tubular systems predominantly depends on the backbone geometrical properties. Interestingly enough, the icosane binding causes the realignment of the H-bond pattern in p(β-T^4_{i+1})$_3$. Not only the tube closing but also all the other H-bonds became of $i \rightarrow (i + 1)$ type. Such an H-bond reshuffling makes a nanotube of a larger inside diameter. Although the system contains a lower number of total H-bonds, it has optimal H-bond parameters ($d_{O-H} = 1.93$Å, $\alpha_{O-H-N} = 164.7°$). Furthermore only one of the three peptide chains adopts A, i.e., a "non-ideal" local fold. As a consequence of the favorable H-bond and backbone geometrical properties the stability of the host−guest complex is significantly higher (+22.6 kcal mol^{-1}) than in p(β-T^4_{i+2})$_3$ type complex. Although these host−guest complexes support that nanotubes are potent encapsulating agents of both polar and apolar molecules, due to steric reasons, 6- or 8-stranded systems are required for drug candidates to be hosted.

By analyzing the dipole moment of these β-nanotubes, one can predict whether it is more suitable to host polar or apolar guest molecules. Twisting of the nanotube increases the dipole moment, the structural effect of which comes from the type of H-bonds connecting the first and last strands. The least screwed parallel and antiparallel nanotubes of an $i \rightarrow (i)$ type H-bond zipper, (β-T^4_i)$_k$, has close to zero dipole moments: μ[p(β-T^4_i)$_4$] = 2.2 D and μ[ap(β-T^4_i)$_4$] = 1.5 D (Table 1). In these nanosystems, the polarization vectors of the H-bonds (partial charges) practically extinguish each other. However, by altering the H-bond zipper the dipole moment increases. For example, in the $i \rightarrow (i + 1)$ type three-stranded parallel nanotubes, the dipole moment is 17.2 D for tripeptide and 21.7 D for tetrapeptide. Similarly, for the antiparallel ap(β-T^3_{i+1})$_k$ nanosystems, with an $i \rightarrow (i + 1)$ zipper, about the same degree of twisting is conserved and highly similar average dipole moments are observed ($\mu = 18.3 \pm 4.0$ D for tripeptide and 25.1 ± 4.0 D for tetrapeptide) (Tables 1 and S5 of Supporting Information). In (β-T^l_{i+2})$_k$ systems, with an $i \rightarrow (i + 2)$ zipper, the value of μ further increases. For parallel, p(β-T^3_{i+2})$_k$, and for antiparallel, ap(β-T^3_{i+2})$_k$, nanotubes the average dipole moment is 31.1 ± 4.4 and 33.6 ± 5.6 D, respectively. When increasing here the number of peptide strands from three to four, the dipole moment can be as high as 43.7 D, ap(β-T^4_{i+2})$_4$, due to the relatively large twisting stabilized by the $i \rightarrow (i + 2)$ zipper. Note that increasing the number of strands result in a higher dipole moment only for the $i \rightarrow (i + 2)$ type nanotubes. In the case of the $i \rightarrow (i + 1)$ type tubular systems the dipole moment of the four-stranded ap(β-T^4_{i+1})$_4$ (23.6 D) is rather similar to the one composed of three-strands only: μ[ap(β-T^3_{i+1})$_4$] = 21.7 D. Enlarging the diameter of the nanotube does not introduce a significant twisting of system, and thus the dipole moment is qualitatively conserved. In contrast, altering the alignment can make a larger difference. The $\Delta\mu$ between parallel and antiparallel nanotubes (e.g., (β-T^4_{i+2})$_4$) can be as large as 7.4 D (Table 1). In conclusion, we have found that the dipole moment of nanotubes changes in a wide range, $1.1 < \mu < 43.7$ D, primarily as a function of the twisting of the polypeptide framework stabilized by the different type of closing H-bond zippers. This indicates that when the type of the H-bond network is in hand the polarity of the nanotube can be controlled by making the system more suitable for accommodating either apolar or polar guest molecules.

In general, the relative stability, ΔE, do not correlate with the polarity of β-Ala nanotubes ($R = 0.01$). However, for the four-stranded nanotubes μ correlates with stability ($R = -0.75$), when normalized by the number of closing H-bonds (Table 1). As mentioned earlier, the largest stabilization energy per H-bond is obtained indeed for the $i \rightarrow (i + 2)$ nanosystems. Here in on one hand the most perfect local H-bond parameters are present and on the other hand the largest tube-twisting is observed giving rise to the highest dipole moment. All these suggest that the primary sequence selection will have a fundamental role in constructing stable apolar or polar nanotubes.

Structural similarities of tropocollagen and β-peptide nanotubes. Tropocollagen, the self-assembled secondary structural element of collagen, has a unique and strictly determined 3D-fold.[35,37] The formation of collagen-like triple helix, a nanotube formed by α-amino acid residues, is commonly associated with the prevalence of POG- and PPG-type sequences. However, collagen consists of several XYG-type subunits, where unlike the amino acid sequence (X,Y ≠ P or O), the overall 3D-fold is preserved.[37] Such a conservative triple helical nanostructure shows similarity in many respects with nanotubes composed of β-peptides, spelled out bellow.

Both in tropocollagen and in β-nanotubes strands are not attached covalently, but are hooked together by $i \rightarrow (i)$ type

TABLE 3: Structural Properties of Tropocollagen and β-Peptide Formed Nanostructures

		collagen model GGG	collagen model AAG	collagen model POG	$(\beta\text{-T}^3_{i+1})_4$	$[\text{ap}((\beta\text{-T}^3_{i+1})_4]_A$	$\text{p}(\beta\text{-T}^4{}_i)_4$	$\text{ap}(\beta\text{-T}^4{}_i)_4$
number of strands		3	3	3	3	3	4	4
H-bond parameters	pattern	$i\rightarrow i$	$i\rightarrow i$	$i\rightarrow i$	$i\rightarrow$ i/H-bond zipper: $i\rightarrow(i+1)$	$i\rightarrow i$/H-bond zipper: $I\rightarrow(i+1)$	$i(\rightarrow)i$/H-bond zipper: $i\rightarrow i$	$i\rightarrow i$/H-bond zipper: $i\rightarrow i$
	d_{O-H}	2.11 ± 0.13[a]	2.06 ± 0.07	2.15 ± 0.15	2.08 ± 0.06[f]	2.19 ± 0.08	2.05 ± 0.06	2.16 ± 0.10
	α_{OHN}	157.7 ± 12.1[b]	158.1 ± 4.9	156.2 ± 3.9	149.8 ± 9.0	147.8 ± 9.9	150.7 ± 6.3	151.1 ± 1.1
backbone dihedral angles	φ	-81.8 ± 18.6[b]	-72.0 ± 17.3	-69.1 ± 10.1	-92.3 ± 2.5, -93.4 ± 1.3, -89.4 ± 7.8	-98.6 ± 6.1, -104.3 ± 9.0, 122.6 ± 25.3	-104.0 ± 5.1, -128.7 ± 43.0, -104.9 ± 1.7, -129.4 ± 46.0	-149.7 ± 0.5, 118.6 ± 1.3, 149.7 ± 0.5, 118.6 ± 1.3
	μ				178.3 ± 0.4, 179.6 ± 0.5, 179.5 ± 0.4	-176.3 ± 7.4, 176.2 ± 2.7, -160.5 ± 9.4	177.5 ± 3.3, 175.0 ± 5.1, 175.0 ± 4.0, 178.0 ± 5.3	177.1 ± 0.8, 171.8 ± 0.5, 177.1 ± 0.8, 171.8 ± 0.5
	Ψ	170.0 ± 43.2	147.0 ± 27.7	147.7 ± 26.8	150.4 ± 1.8, 149.5 ± 0.4 150.5 ± 2.9	151.1 ± 14.3, 154.8 ± 4.0, -103.8 ± 37.0	126.5 ± 1.9, 155.1 ± 47.0 129.7 ± 8.1, 152.8 ± 42.4	149.5 ± 1.1, 121.8 ± 4.8, 149.5 ± 1.1, 121.8 ± 4.8
dihedral angle of neighboring amide C═O groups[c]		-112.0	-101.0	-108.8	47.8	36.7	12.8	0
diameter of "tubes"		5.6[a]	5.7	5.7	5.5	5.3	6.2	6.2
average pitch of the strands[d]		9.0[a]	9.4	9.5	10.8	11.0	10.9	10.9
chirality of the strands		M[e]	M	M	P	P	P	0

[a] All distances in Å. [b] All values in degrees. [c] The dihedral angles were determined by $O_i-C_i'-C_{i+1}'-O_{i+1}$ atoms. [d] Average distance between the ith and $(i+9)$th backbone atom in one strand in Å. [e] M and P symbol was used for strands show negative and positive chirality, respectively. One of the tubes, the $\text{ap}(\beta\text{-T}^4{}_i)_4$ does not show any chirality, and therefore its symbol is 0. [f] For parallel nanotubes, the geometrical properties are taken from ref 2.

H-bonds. As long as, in collagen, the unique $i \rightarrow (i)$ type H-bond pattern is present, in β-nanotubes, several (e.g., $i \rightarrow (i)$, $i \rightarrow (i + 1)$, $i \rightarrow (i + 2)$) H-bond variants could be observed. Furthermore, in tropocollagen, only every third, whereas in β-nanotubes, each and every amide NHs and COs are part of an H-bond. In conclusion, although the H-bond pattern can be very similar for both types of supramolecular systems, typically three stranded β-peptide nanotubes contain three times more hydrogen bonds than collagen does (Figure 1, see the black and the grey dashed lines). When comparing their H-bond parameters, the O···H distances can be quite similar. For example, the d_{O-H} values are 2.06 ± 0.07 Å for collagen composed of AAG triplets[37] and 2.08 ± 0.06Å for the corresponding three-stranded β nanotube $\text{p}(\beta\text{-T}^3{}_{i+1})_4$ (Table 3). Although the H-bond angles can be slightly different ($\Delta\alpha \approx 9°$), in general, the geometrical properties of their H-bond networks resemble a lot.

By examining the backbone torsional angles [φ, Ψ] for collagen and [φ, μ, Ψ] for β-nanotubes, a great similarity is detected for the two systems. For example, for the three stranded $\text{p}(\beta\text{-T}^3{}_{i+1})_4$, $\varphi \sim -90°$, $\mu \sim 180°$, $\Psi \sim 150°$, while for the most flexible GGG type tropocollagen, $\varphi \sim -80°$ and $\Psi \sim 170°$. By consideration of the close to 180° typical values of μ, the overall twisting of the polypeptide chains can indeed be very similar both for the α- and for the β-peptide nanosystems. For β-nanotubes which contain more than three strands, the similarity of the φ and Ψ values with the collagen-like triple helices is slightly lower: e.g., for $\text{p}(\beta\text{-T}^4{}_i)_4$ and $\text{p}(\beta\text{-T}^4{}_{i+1})_4$, the difference is around 30° (Table 3).

When comparing their macroscopic parameters the similarity of the three-stranded β-nanotube and of the tropocollagen is striking. For example, the inside diameters of collagen is ∼5.65 Å and this data is ∼5.4 Å for the three-stranded nanotubes (Table 3). Furthermore, the average distance between the ith and $(i + 10)$th backbone atoms of a strand is just slightly larger for the β-nanotube (10.8 Å) than it is for the collagen (9.0−9.5 Å) (Table 3). Considerable difference can only be observed in the twist of the adjacent amide groups: the dihedral angle formed by two neighboring amide C═O groups (i.e., by the $O_i-C_i'-C_{i+1}'-O_{i+1}$ atoms) is −112.0° for GGG and −101.1° for AAG collagen models, whereas the value is around 37° in $\text{p}(\beta\text{-T}^3{}_i)_4$. Finally, the twisting of a collagen forming strand is minus, M, while it is plus, P, for most β-nanotubes.

In conclusion, we have found that the structural characteristics of nanotubes, formed by β-peptides and by collagen, are similar. The strong resemblance of their basic geometrical, H-bond, and dihedral angle parameters suggests that they can be regarded as supramolecular complexes of common roots. In other words, β-nanotubes are the non-natural variants of collagen like secondary structural elements having, however, a more versatile nature.

Conclusion

We have investigated the nanotube forming properties of multiple-stranded β-peptides. A comprehensive structure elucidation study was accomplished on a set of β-peptides $[CH_3CO-(\beta\text{-Ala})_k-NH-CH_3]_l$ $(2 \le k \le 4, 2 \le l \le 4)$ by using both ab initio and DFT calculations. We have found that both the three- and the four-stranded supramolecular systems can form both parallel and antiparallel β-nanotubes. The four-stranded model can adopt at least three different types of antiparallel tubular systems, namely, $\text{ap}(\beta\text{-T}^4{}_i)_k$, $\text{ap}(\beta\text{-T}^4{}_{i+1})_k$,

and ap(β-T$^4_{i+2}$)$_k$, where ($i + x$) refers to the hydrogen bonding pattern operative between the first and the last strands. The three-stranded superstructure was found to form at least two different nanotubes, namely, ap(β-T$^3_{i+1}$)$_k$ and ap(β-T$^3_{i+2}$)$_k$. For three-stranded tubular structures, two out of the three chains must always be aligned in parallel, and thus a total of three different subtypes, A, B, and C, were assigned and characterized both for ap(β-T$^3_{i+2}$)$_k$ and for ap(β-T$^3_{i+1}$)$_k$.

Both for the parallel and the antiparallel nanotubes, the ideal local fold is that of S_P, a slightly spiral backbone structure. Although the dihedral angles of the individual peptide chains can be somewhat distorted from their ideal fold, the more their local conformation resembles to Sp the higher their stability is. The overall stability further depends on the geometrical parameters of interchain hydrogen bonds holding the tertiary structures together. In those tubular systems, where the length of O···H distances are short and the α_{O-H-N} angles are close to what is in extended β-layers, the relative stability is high. In addition, the overall stability of these nanotubes increases with the number of the polypeptide strands and with the length of each polypeptide chains incorporated. The antiparallel four-stranded ap(β-T$^4_{i+1}$)$_4$ tubular system turns out to be the most stable secondary structure element among all investigated antiparallel supramolecular complexes with a relative stability of -30.1 kcal mol^{-1} compared to ap(β-E^4)$_4$. Even though very stable, its electronic energy is still higher by some 10 kcal mol^{-1} than that of the appropriate "full-parallel" β-peptide nanotube, p(β-T$^4_{i+1}$).

Altering the H-bond zipper modifies the polarity of a nanotube. Drug delivery abilities of nanotubes were studied by using small organic molecules such as water, acetonitrile, and an alkane placed inside a three- and a four-stranded nanotube. Followed by full geometry optimization, we have found that only the four-stranded systems, e.g., p(β-T$^4_{i+1}$)$_k$, ap(β-T$^4_{i+1}$)$_k$, and ap(β-T$^4_{i+2}$)$_k$, which have the largest tube diameter, can incorporate in an intact manner these guest molecules. This suggests that both parallel and antiparallel nanotubes composed of at least six strands could be suitable hosts and used as potential drug delivery systems.

In order to study the effect of environment on the affinity of tube formation, supporting computations were performed for both parallel and antiparallel four-stranded β-nanotubes using IEFPCM model.[42,43] In line with the expectations, the nanotubes have higher stability than the extended-like β-layer only in apolar (e.g., membrane) environment.

Single point energy calculations of four-stranded tubular structures were also performed using X3LYP functional, which was developed to describe van der Waals (vdW) interactions better.[48] We found, that each nanotube gained an additional $\sim$3$-$4 kcal/mol^{-1} stability.

The role of chirality was also examined using nanotube models containing the β-Abu and β-Aib amino acid residues, respectively. This way, it was tested whether amino acids with side chains on the second carbon (β-Aib-type residues) or amino acids with side chains on the third carbon (β-Abu-type residues) are more suitable to form such nanotubes. We concluded that β-amino acids with β-Abu-like side chains are much more preferred.

Finally, the tubular shape of the collagen-like triple-helices and β-nanotubes show similarities in many respects. We have found that both their H-bond geometrical and pairing properties are similar. As long as collagen-like triple helices are conservative structures having an $i \rightarrow (i)$ type H-bond pattern only, β-nanotubes are more versatile and can have either an $i \rightarrow (i)$, $i \rightarrow (i + 1)$ or $i \rightarrow (i + 2)$ type H-bonds zippers. Due to the additional backbone methylene group of β-amino acids, the latter types of supramolecular complexes are more flexible. Consequently, unlike in collagen, all C═O acceptor and NH donor groups of β-nanotubes are oriented such that they are part of an interchain H-bond. Despite of their similar H-bond pattern, some geometrical properties of these tubular structures can be slightly different. Nevertheless, β-nanotubes can be regarded as non-natural representatives of tropocollagen. It is hoped that the present structural and energetic properties of these supramolecular nanosystems will aid the design of novel, self-assembling bioactive peptide derivatives.

Abbreviations List

β-Peptide, peptide composed of β-amino acids; T, tube; E, extended β-layer; DFT, density functional theory; S_P, spiral backbone conformation of β-amino acids with torsional angles φ = *gauche minus*, μ = *anti*, and Ψ = *anti* (g^-aa); S^*_P, spiral backbone conformation of β-amino acids (aag^-)^1; β-nanotube, a nanotube composed of β-peptide strands interconnected by hydrogen bonds; Abu, 3-aminobutanoic acid; Aib, 3-aminoisobutanoic acid; O, hydroxyl-Pro.

Acknowledgment. The help of Villõ Pálfi and Gábor Pohl is highly appreciated. The work has been performed under the Project HPC-EUROPA (RII3-CT-2003-506079), with the support of the European Community - Research Infrastructure Action under the FP6 "Structuring the European Research Area" Programme. This work was also supported by grants from the Hungarian Scientific Research Fund (OTKA K72973, NI68466), MediChem2, and ICGEB (Hun04-03). The ELTE computer facility and the HPC group, U. Szeged, were used for several computations. Authors would like to dedicate this work to Prof. Tamás Vajda on the occasion of his 80th birthday.

Supporting Information Available: Geometric properties of the nanotubes computed at RHF/3$-$21G and at B3LYP/6$-$31G(d) level of theory; structural, energetic properties, and H-bond parameters of tripeptide nanotubes computed at B3LYP/6$-$31G(d) level of theory; energetic properties of tetrapeptide tubular systems using implicit solvent (IEFPCM) computed at B3LYP/6$-$31G(d) level of theory. This material is available free of charge via the Internet at http://pubs.acs.org.

References and Notes

(1) Seebach, D.; Beck, A. K.; Bierbaum, D. J. *Chem. Biodiversity* **2004**, *1*, 1111.
(2) Beke, T.; Csizmadia, I. G.; Perczel, A. *J. Am. Chem. Soc.* **2006**, *128*, 5158.
(3) Gellman, S. H. *Abstr.Pap.— Am. Chem. Soc.* **1999**, *217*, U160.
(4) Porter, E. A.; Wang, X. F.; Schmitt, M. A.; Gellman, S. H. *Org. Lett.* **2002**, *4*, 3317–3319.
(5) Appella, D. H.; Christianson, L. A.; Klein, D. A.; Powell, D. R.; Huang, X. L.; Barchi, J. J.; Gellman, S. H. *Nature* **1997**, *387*, 381–384.
(6) Porter, E. A.; Weisblum, B.; Gellman, S. H. *J. Am. Chem. Soc.* **2002**, *124*, 7324–7330.
(7) Frackenpohl, J.; Arvidsson, P. I.; Schreiber, J. V.; Seebach, D. *ChemBioChem* **2001**, *2*, 445–455.
(8) Hintermann, T.; Seebach, D. *Chimia* **1997**, *51*, 244–247.
(9) Seebach, D.; Albert, M.; Arvidsson, P. I.; Rueping, M.; Schreiber, J. V. *Chimia* **2001**, *55*, 345–353.
(10) Seebach, D.; Abele, S.; Gademann, K.; Guichard, G.; Hintermann, T.; Jaun, B.; Matthews, J. L.; Schreiber, J. V. *Helv. Chim. Acta* **1998**, *81*, 932–982.
(11) Martinek, T. A.; Toth, G. K.; Vass, E.; Hollosi, M.; Fulop, F. *Angew. Chem., Int. Ed.* **2002**, *41*, 1718–1721.
(12) Seebach, D.; Overhand, M.; Kuhnle, F. N. M.; Martinoni, B.; Oberer, L.; Hommel, U.; Widmer, H. *Helv. Chim. Acta* **1996**, *79*, 913–941.

(13) Seebach, D.; Abele, S.; Gademann, K.; Jaun, B. *Angew. Chem., Int. Ed.* **1999**, *38*, 1595–1597.
(14) Krauthauser, S.; Christianson, L. A.; Powell, D. R.; Gellman, S. H. *J. Am. Chem. Soc.* **1997**, *119*, 11719–11720.
(15) Karle, I.; Gopi, H. N.; Balaram, P. *Proc. Natl. Acad. Sci. U.S.A.* **2002**, *99*, 5160–5164.
(16) Chung, Y. J.; Huck, B. R.; Christianson, L. A.; Stanger, H. E.; Krauthauser, S.; Powell, D. R.; Gellman, S. H. *J. Am. Chem. Soc.* **2000**, *122*, 3995–4004.
(17) Diederichsen, U.; Schmitt, H. W. *Eur. J. Org. Chem.* **1998**, 827–835.
(18) Chung, Y. J.; Christianson, L. A.; Stanger, H. E.; Powell, D. R.; Gellman, S. H. *J. Am. Chem. Soc.* **1998**, *120*, 10555–10556.
(19) Daura, X.; Gademann, K.; Schafer, H.; Jaun, B.; Seebach, D.; van Gunsteren, W. F. *J. Am. Chem. Soc.* **2001**, *123*, 2393–2404.
(20) Gunther, R.; Hofmann, H. J.; Kuczera, K. *J. Phys. Chem. B* **2001**, *105*, 5559–5567.
(21) Beke, T.; Somlai, C.; Perczel, A. *J. Comput. Chem.* **2006**, *27*, 20–38.
(22) Beke, T.; Csizmadia, I. G.; Perczel, A. *J. Comput. Chem.* **2004**, *25*, 285–307.
(23) Möhle, K.; Gunther, R.; Thormann, M.; Sewald, N.; Hofmann, H. J. *Biopolymers* **1999**, *50*, 167–184.
(24) Langenhan, J. M.; Guzei, I. A.; Gellman, S. H. *Angew. Chem., Int. Ed.* **2003**, *42*, 2402–2405.
(25) Lin, J. Q.; Luo, S. W.; Wu, Y. D. *J. Comput. Chem.* **2002**, *23*, 1551–1558.
(26) Banerjee, I. A.; Yu, L.; Matsui, H. *Proc. Natl. Acad. Sci. U.S.A.* **2003**, *100*, 14678.
(27) Ghadiri, M. R.; Granja, J. R.; Buehler, L. K. *Nature* **1994**, *369*, 301.
(28) Djalali, R.; Samson, J.; Matsui, H. *J. Am. Chem. Soc.* **2004**, *126*, 7935–7939.
(29) Clark, T. D.; Buehler, L. K.; Ghadiri, M. R. *J. Am. Chem. Soc.* **1998**, *120*, 651–656.
(30) Bolter, B.; Soll, J. *EMBO J.* **2001**, *20*, 935–940.
(31) Kleinschmidt, J. H. *Cell. Mol. Life Sci.* **2003**, *60*, 1527–1528.
(32) Karplus, P. A.; Daniels, M. J.; Herriott, J. R. *Science* **1991**, *251*, 60–66.
(33) Locher, K. P.; Rees, B.; Koebnik, R.; Mitschler, A.; Moulinier, L.; Rosenbusch, J. P.; Moras, D. *Cell* **1998**, *95*, 771–778.
(34) Orgel, J. P. R. O.; Irving, T. C.; Miller, A.; Wess, T. J. P. *Proc. Natl. Acad. Sci. U.S.A.* **2006**, *103*, 9001–9005.
(35) Bhattacharjee, A.; Bansal, M. *IUBMB Life* **2005**, *57*, 161–172.
(36) Baum, J.; Brodsky, B. *Folding Des.* **1997**, *2*, R53–R60.
(37) Pálfi, V. K.; Perczel A. *J. Comput. Chem.* in press.
(38) Beke, T.; Czajlik, A.; Balint, B.; Perezel, A. *ACS Nano.* **2008**, *2*, 545–553.
(39) Hamada, N.; Sawada, S.; Oshiyama, A. *Phys. Rev. Lett.* **1992**, *68*, 1579–1581.
(40) Asthagiri, D.; Bashford, D. *Biophys. J.* **2002**, *82*, 1176–1189.
(41) Frisch, M. J.; et al. Gaussian, Inc.: Wallingford, CT, 2004.
(42) Perczel, A.; Hudáki, P.; Füzéry, A. K.; Csizmadia, I. G. *J. Comput. Chem.* **2004**, *25*, 1084–1100.
(43) Cances, E.; Mennucci, B.; Tomasi, J. *J. Chem. Phys.* **1997**, *107*, 3032–3041.
(44) Mennucci, B. Tomasi, J. *J. Chem. Phys.* **1997**, *106*, 5151–5158.
(45) Allen, M.; Tozer, D. J. *J. Chem. Phys.* **2002**, *117*, 11113–11120.
(46) Zimmerli, U.; Parrinello, M.; Koumoutsakos, P. *J. Chem. Phys.* **2004**, *120*, 2693–2699.
(47) Tsuzuki, S.; Luethi, H. P. *J. Chem. Phys.* **2001**, *114*, 3949–3957.
(48) Xu, X.; Goddard, W. A. *Proc. Natl. Acad. Sci. U.S.A.* **2004**, *101*, 2673–2677.

JP7114803